ACS OMEGA

http://pubs.acs.org/journal/acsodf

Article

Determining the Predominant Conformations of Mortiamides A−D in Solution Using NMR Data and Molecular Modeling Tools

Tanos C. C. Franca, Arlan da Silva Goncalves, Christopher Bérubé, Normand Voyer, Norman Aubry, and Steven R. LaPlante*

Cite This: *ACS Omega* 2023, 8, 25832−25838

Read Online

ACCESS | Metrics & More | Article Recommendations | Supporting Information

ABSTRACT: Macrocyclic peptidomimetics have been seriously contributing to our arsenal of drugs to combat diseases. The search for nature's discoveries led us to mortiamides A−D (found in a novel fungus from Northern Canada), which is a family of cyclic peptides that clearly have demonstrated impressive pharmaceutical potential. This prompted us to learn more about their solution-state properties as these are central for binding to target molecules. Here, we secured and isolated mortiamide D, and then acquired high-resolution nuclear magnetic resonance (NMR) data to learn more about its structure and dynamics attributes. Sets of two-dimensional NMR experiments provided atomic-level (through-bond and through-space) data to confirm the primary structure, and NMR-driven molecular dynamics (MD) simulations suggested that more than one predominant three-dimensional (3D) structure exist in solution. Further steps of MD simulations are consistent with the finding that the backbones of mortiamides A−C also have at least two prominent macrocyclic shapes, but the side-chain structures and dynamics differed significantly. Knowledge of these solution properties can be exploited for drug design and discovery.

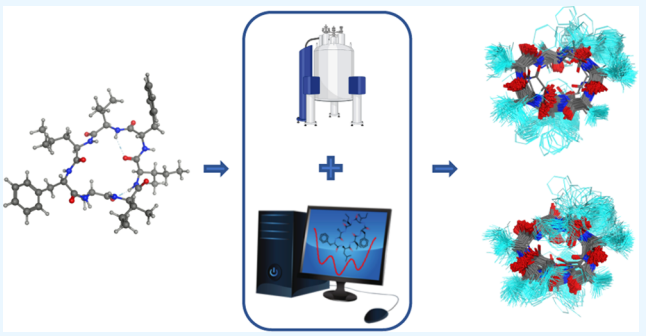

INTRODUCTION

Mortiamides A−D (Figure 1) are four related cyclic heptapeptides composed of a mixture of D/L hydrophobic amino acids. They were first identified by Grunwald et al.[1] in a novel fungus of the genus *Mortierella* sp., which was found in marine sediments obtained in Northern Canada. Prompted by their structural similarities to other natural macrocyclic peptides with anti-plasmodial activities,[2] mortiamides A−D were tested for activity against *Plasmodium falciparum* chloroquine−mefloquine−pyrimethamine multiresistant strains, by Bérubé et al.[3] Interesting levels of activities were observed against *P. falciparum* with an IC_{50} of 5.3 μM for mortiamide A, 2.1 μM for mortiamide B, 0.94 μM for mortiamide D, and a surprising lack of activity for mortiamide C at similar concentrations tested (Figure 1).

The different activities noted for mortiamides A−C suggested that a better understanding of the solution properties was warranted. The fact that they were composed of a mixture of D and L hydrophobic amino acids linked via a macrocycle made the study more intriguing. Moreover, we were interested in extracting any potential design ideas given that trends in structure−activity relationships (SAR) were noted—D is 5 times more potent than A, B has intermediate activity, and C is inactive. Given that the solution properties of compounds are central for binding to target proteins, we aimed to determine the solution conformations of these mortiamides to explore how they may be related to the observed SAR.

However, determining the predominant conformational structures of macrocycles, like mortiamides A−D, compatible with experimental data, is not an easy task. For this kind of molecule, thousands of distinct conformations with local minima energies very close to the global minima are possible. This turns the work of finding the exact conformer corresponding to the experimental data exhausting and time-consuming.[4]

In addition to the X-ray data, not always available, experimental information for the elucidation of 3D structures of macrocycles is usually obtained from NOE-derived NMR experiments with ^3J-coupling torsional restraints and experimentally determined distances. These results can feed conformational search methods meant to point to the low-energy conformers that will fit those distances the most.[4] However, the dynamicity of the NMR data, which normally represent a compilation of many interconverting conformers,

Received: February 22, 2023
Accepted: June 7, 2023
Published: July 11, 2023

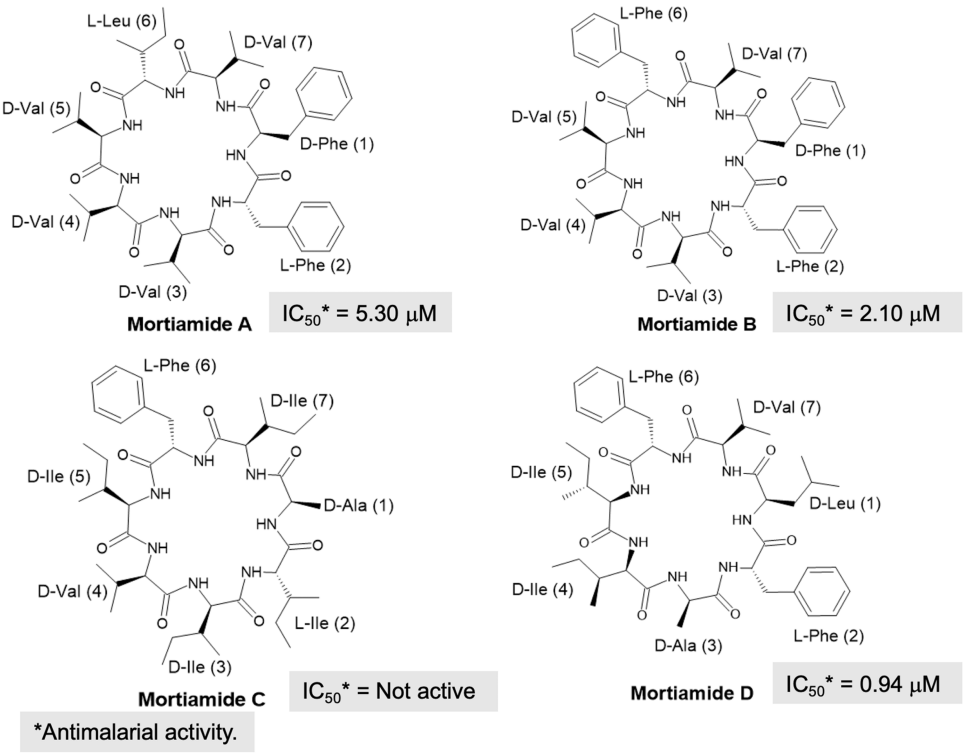

Figure 1. 2D structures of mortiamides A−D with their respective antimalarial activities.

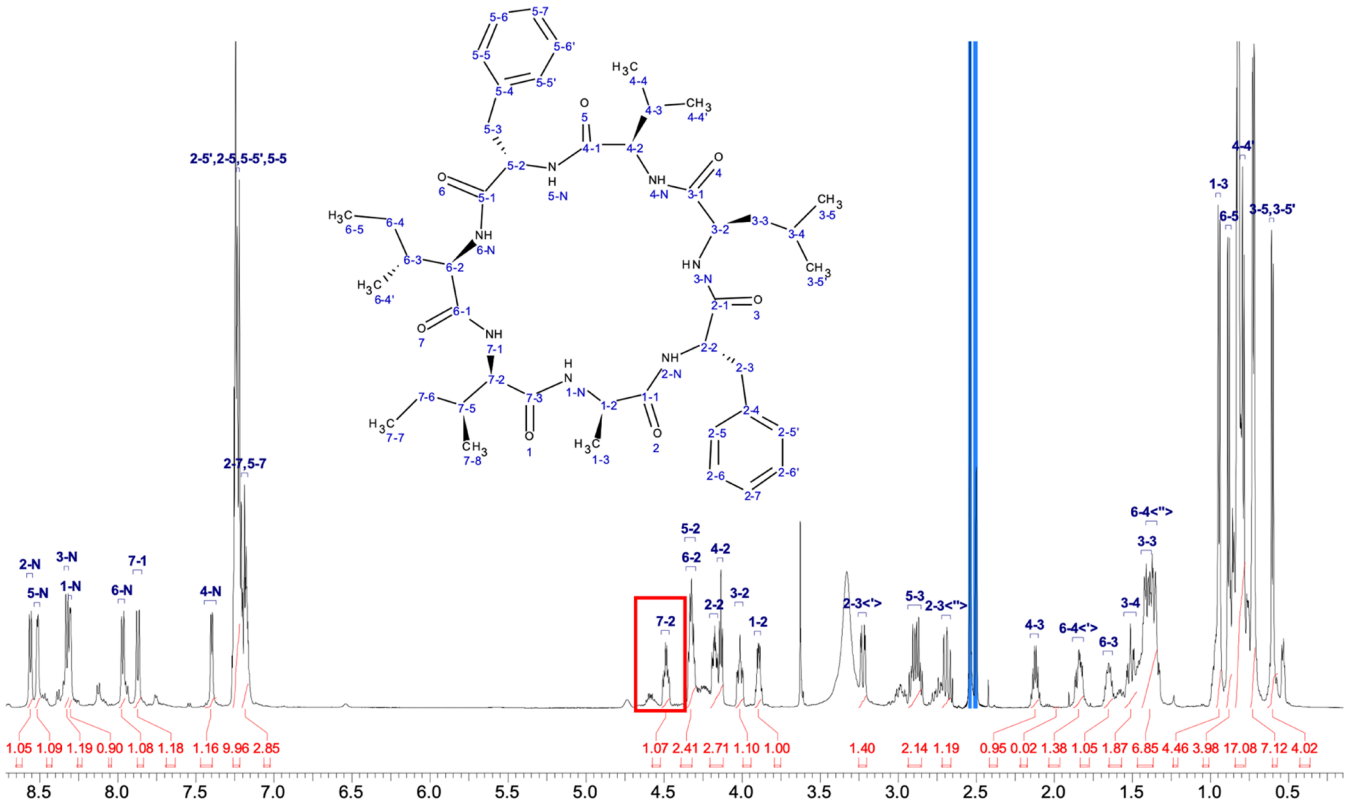

Figure 2. ^{1}H NMR spectra of mortiamide D.

can make it difficult to find one conformer matching all constraints/distances or, instead, point to multiple matching conformers.[4,5] To solve this problem, many NMR and modeling strategies have been assessed.[6]

Usually a combination of techniques is necessary to access the conformational complexity of a macrocycle[4] once standardized methods are scarce, under development, or not available in open-access software. Therefore, most of the approaches currently found in the literature combine

https://doi.org/10.1021/acsomega.3c01206
ACS Omega 2023, 8, 25832−25838

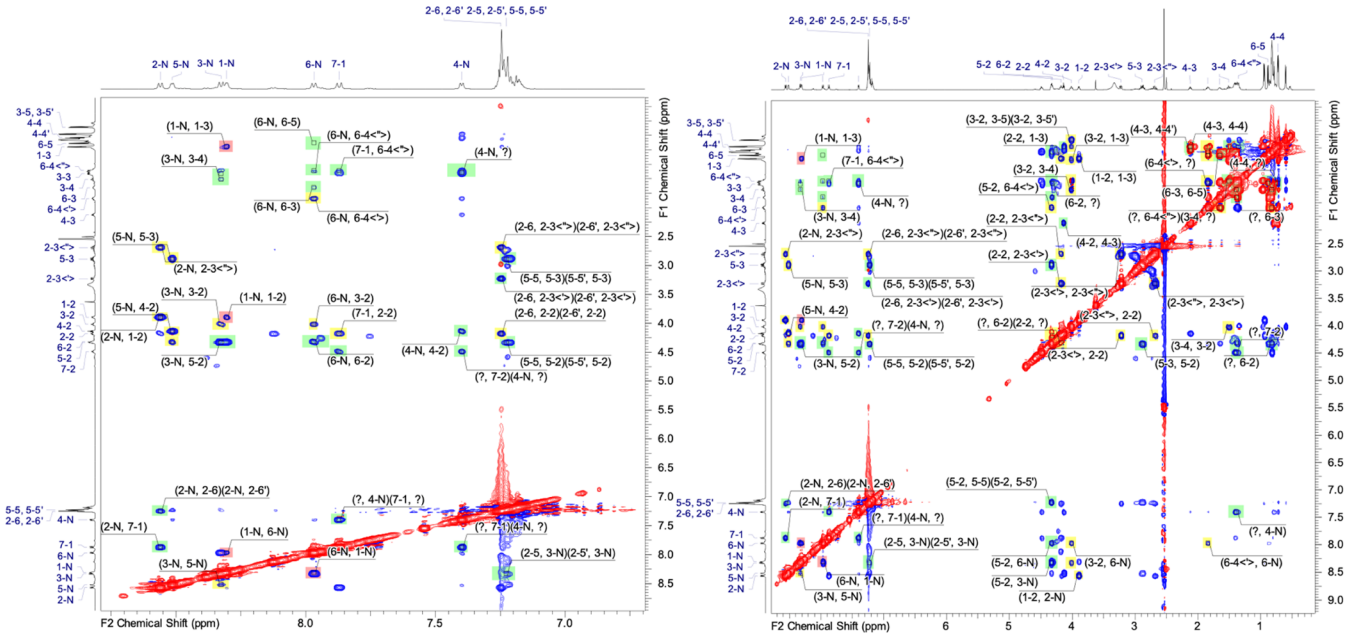

Figure 3. ROESY NMR spectra of mortiamide D.

Table 1. NOE NMR Assignments of the Atom Pairs Selected to be Monitored in the Theoretical Studies (Extracted from Table S1) and the Corresponding 2D Structures of Mortiamide D with the Atoms Labeled (Left) and the Pairs Distances Shown in Green Arrows (Right)

F2 (ppm)	F1 (ppm)	F2 Range (ppm)	F1 Range (ppm)	Abs. Volume	Type	Strength	Assignments
8.33	4.33	[8.28 .. 8.35]	[4.27 .. 4.38]	13.498	NOE	strong	3-N, 5-2
3.90	8.56	[3.88 .. 3.91]	[8.54 .. 8.58]	3.902	NOE	medium	1-2, 2-N
7.97	8.30	[7.95 .. 7.99]	[8.28 .. 8.36]	4.881	NOE	medium	6-N, 1-N
8.51	4.14	[8.50 .. 8.53]	[4.12 .. 4.15]	3.261	NOE	medium	5-N, 4-2
8.56	7.87	[8.54 .. 8.58]	[7.84 .. 7.91]	2.490	NOE	medium	2-N, 7-1(7-N)
4.01	7.97	[3.99 .. 4.05]	[7.93 .. 8.00]	1.488	NOE	weak	3-2, 6-N
7.87	4.18	[7.85 .. 7.89]	[4.14 .. 4.22]	1.790	NOE	weak	7-1, 2-2
8.33	8.51	[8.31 .. 8.34]	[8.49 .. 8.53]	0.560	NOE	weak	3-N, 5-N

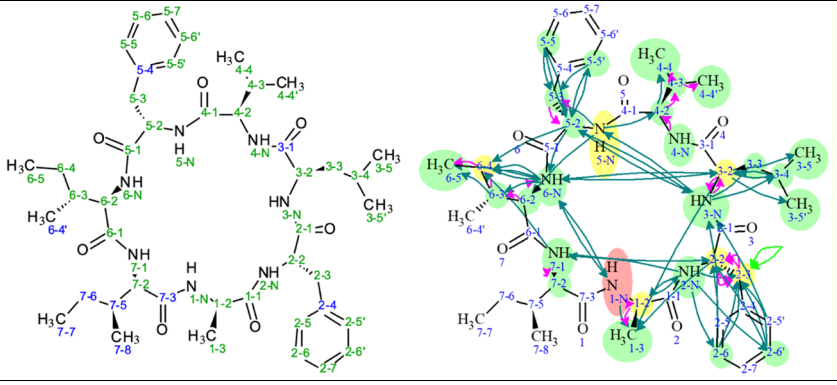

optimization methods, search algorithms, and MD simulation techniques using different force fields in order to probe the most the energy surface. This increases the chances of successfully crossing the barriers among local minima and identifying the global minimum or the minima corresponding to the experimental data available.[7]

Standard algorithms meant to exploring the macrocycle conformational space have also been developed and implemented in molecular modeling software packages. Some examples are the LowModeMD sampling algorithm,[8] which is part of the conformational search module of MOE (https://www.chemcomp.com/Products.htm), and the Prime-MCS[9] developed for the Schrödinger package (https://www.schrodinger.com/). Those methods have been tried face to several databases of macrocycles with different sizes and showed to be capable of predicting, with a quite good accuracy, the conformations of X-ray structures, with the advantage of

https://doi.org/10.1021/acsomega.3c01206
ACS Omega 2023, 8, 25832−25838

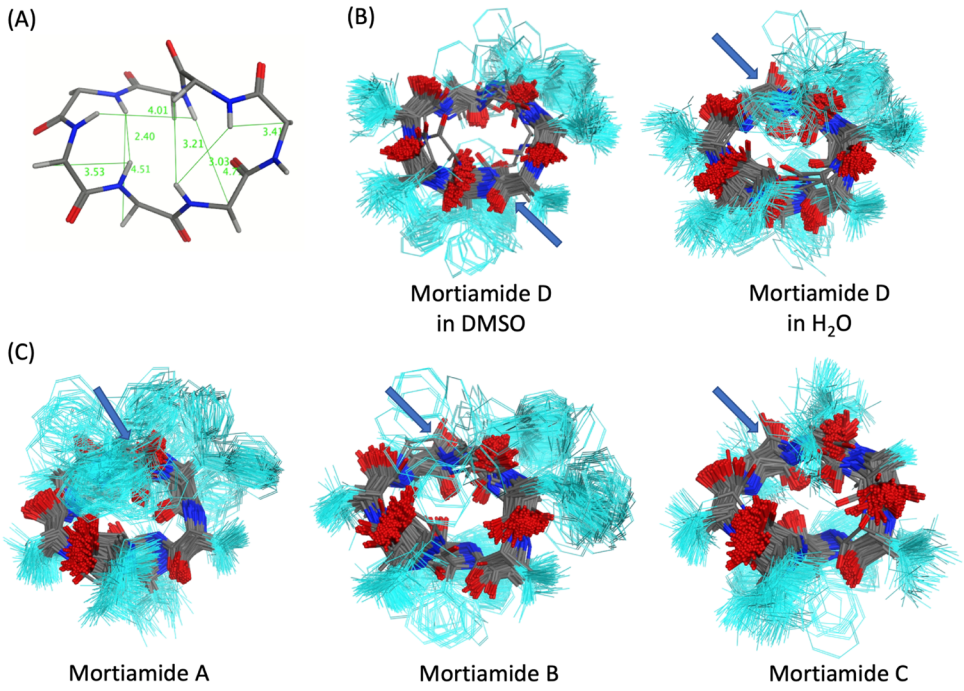

Figure 4. (A) Backbone of the mortiamide D conformer obtained after running the LowModeMD sampling algorithm of MOE (https://www.chemcomp.com/Products.htm). The distances in Å corresponding to the assignments in Table 1 are shown in green lines. Side chains were omitted to facilitate visualization. (B) Superposition of frames of the predominant conformer of mortiamide D, collected at each 1 ns of MD simulation in DMSO and H_2O. (C) Superpositions of frames of mortiamides A−C conformers, collected at each 1 ns of MD simulation in H_2O. Backbones are shown in sticks, while side chains are shown in wire and colored in light blue. Inverted peptide bonds are pointed by arrows.

being much faster and user friendly, besides demanding less hardware resources.

In this work, we used a combination of NMR spectroscopy, the LowModeMD sampling algorithm[8] of MOE (https://www.chemcomp.com/Products.htm), and molecular dynamics (MD) simulations to find the predominant solution conformations of mortiamide D. Structural modifications of this conformer, followed by additional steps of free MD simulations, enabled also the theoretical prediction of the predominant solution conformations of mortiamides A−C.

RESULTS

NMR Spectroscopy Data and Structure Assignments. Our strategy for probing the predominant solution conformations of the mortiamide compounds first employed NMR spectroscopy to secure experimental conformational information at the atomic level. For this, we focused our experimental approach by securing a concentrated sample of mortiamide D and then acquiring a series of one- and two-dimensional NMR spectra at 600 MHz.

NMR resonance assignments were determined using a combination of ^{1}H 1D and ROESY NMR spectra (Figures 2 and 3) along with ^{13}C 1D, COSY, TOCSY, HSQC−DEPT, and HMBC NMR spectra (Figures S1−S5). It is noteworthy that two states are observable in the NMR data (see red box in Figure 2). Here, we focus on the predominant free-state conformation. The resonance assignments are shown in Figures 2 and 3 and a complete listing is provided in the Supporting Information. Overall, the complete resonance assignments are fully consistent with the proposed primary structure shown in Figure 1.

Information regarding the predominant conformation adopted by mortiamide D was then extracted from J-coupling constants (torsion angle information) and from ROESY cross-peaks (inter-hydrogen distance information). Figure 3 provides a view of the assignments of the observed ROESY cross-peaks (see also Table S1).

The subset of the ROESY data, corresponding to the distances between protons present in the backbone of mortiamide D, which are the ones relevant for the conformational analysis, was then extracted to initiate computational studies for an overview of 3D structures that are consistent with the NMR data. Table 1 provides a listing of NMR information, which included the critical ROESY cross-peaks whose relative strengths were translated to inter-hydrogen distance restraints in the 3D structure simulations. Also, the 2D structure of mortiamide D with the atoms labeled and arrows between hydrogens for which noteworthy ROESY cross-peaks were observed are shown.

The strong, medium, and weak ROESY cross-peaks were employed as ranges of distance restraints in the calculations: 2.2−3.2 Å for the strong, 3.3−4.0 Å for the medium, and 4.0−4.5 Å for the weak cross-peaks. See also Figure S6 which shows the ensemble of inter-hydrogen distance information (shown by the red arrows).

Computational Chemistry Modeling of the NMR Data for Mortiamide D. The first predominant conformer of mortiamide D was determined using the LowModeMD sampling algorithm,[8] of MOE (https://www.chemcomp.com/Products.htm), as described in the Methodology section, until achieving the conformer, which backbone is shown in Figure 4A, matching the most the ranges of distances predicted by the assignments listed in Table 1. This conformer was further submitted to MD simulations using the AMBER10:-EHT[10] forcefield in order to assess its dynamic stability. The comparison between NMR-predicted and LowModeMD-

https://doi.org/10.1021/acsomega.3c01206
ACS Omega 2023, 8, 25832−25838

calculated distances shown in Table S2 reveals that most of them are below the limit pointed out by the NMR experiments. Minor errors of 2.7 and 1.3% were observed for assignments 1-2, 2-N and 7-1, 2-2, respectively, while the major difference was observed for assignment 3-N, 5-2 with 28.4% of error.

The plots of root-mean-square deviation (RMSD) of mortiamide D during the MD simulations in both water and DMSO are shown in Figure S7, while the superpositions of frames collected at each 1 ns of MD simulation are shown in Figure 4B. Analysis of the frames in Figure 4B suggests that the existence of more than one predominant conformation (see backbones in Figure S8) resulting from interconversion of some dihedrals is possible. The frequency of these inversions can be visualized in the plots of variation of the dihedral angles of mortiamide D during the MD simulations shown in Figure S9.

Computational Chemistry Modeling of the Predominant Conformers of Mortiamides A−C. The predictions of the predominant conformers of mortiamides A−C in solution were performed based on mutations on the first predominant conformer obtained for mortiamide D. The protein builder tool of MOE (https://www.chemcomp.com/Products.htm) was used in order to obtain the structure of each mortiamide, followed by validation through MD simulation. The RMSD plots obtained during the MD simulations are shown in Figure S11, while the superpositions of frames collected at each 1 ns of MD simulation are shown in Figure 4C. Similar to mortiamide D, the MD simulations also point to the possible existence of more than one prevalent conformation as shown in the superpositions of frames and plots of variation of dihedral angles in Figures S11 and S12.

DISCUSSION

The mortiamide D conformer obtained through the LowModeMD conformational search, whose backbone is shown in Figure 4A, brings all NOE assignments compatible with the distances predicted by the NOE NMR assignments in Table 1, satisfying all cross-peaks corresponding to the strong, medium, and weak interactions, with very slight variations in some cases. Also, the RMSD plots during the MD simulations (Figure S7) in DMSO and water obtained for our mortiamide D conformer show stability since the beginning of the simulations with values of the backbones never passing 2.00 Å for the backbones and 5.00 Å for the main chain. These results, together with the overlap of frames shown in Figure 4B, point to the stabilization of the conformers during the MD simulations in both solvents. As can be seen in Figure S11, more than one predominant conformer is possible, and our MD results also suggest that the two distinct solvents (DMSO and water) seem to favor the distinct conformers of mortiamide D in solution.

The RMSD plots for the predicted conformers of mortiamides A−C shown in Figure S10 also pointed to the stabilization of the systems since the beginning of the simulation and compatibility with an NMR-solved macrocycle structure. Similar to mortiamide D, the RMSD never passed 2.00 Å for the backbone and 5.00 Å for main chain in all three cases. Also, the possible existence of more than one predominant conformer in solution was pointed for mortiamides A−C (see Figures S11 and S12).

CONCLUSIONS

In this work, we used the LowModeMD sampling algorithm[8] of MOE (https://www.chemcomp.com/Products.htm), to find the low-energy conformers of mortiamide D matching the most to the constraints and cross-peaks between protons determined through ROESY NMR experiments. The results obtained converged to a low-energy conformer compatible with the NMR data. Further 200 ns of free molecular dynamics (MD) simulations confirmed the stability of this conformer and suggested the existence of more than one predominant similar conformer due to inversion peptide bonds. Structural modifications of the conformer compatible with the NMR data, followed by 200 ns of free MD simulations, enabled also the theoretical prediction of the predominant conformers of mortiamides A−C in solution.

In conclusion, our studies enabled finding the predominant conformers of mortiamide D, besides the prediction of the possible predominant conformers of mortiamides A−C in solution. The MD simulation studies allowed us to infer that the backbones of the 4 mortiamides have a common prominent macrocyclic shape. This suggests that the different antimalarial activities observed for these compounds are most likely due to their different side chains whose orientations should be the factor changing the fitting of these molecules in the binding pocket of their corresponding molecular target. We propose that the bioactive free-state conformation described herein can be amenable for structure-dynamics-based drug discovery efforts[11]

METHODOLOGY

Sample of Mortiamide D. The mortiamide D sample used in this study was synthesized and purified in-house following the same procedure described before.[3]

NMR Experiments. The NMR spectra of ^{1}H, ^{13}C, COSY, TOCSY, HSQC−DEPT, HMBC, and ROESY were obtained in a Bruker 600 MHz spectrometer from the mortiamide D sample mentioned above. This sample was dissolved in DMSO-d6 and the NMR experiments were performed according to in-house protocols described before.[12] The spectrum module from the Advanced Chemistry Development, Inc. (ACD/Labs) (https://www.acdlabs.com/company/reference.php) was used to determine the assignments of the peptide using the COSY, TOCSY, HSQC−DEPT, and HMBC experiments, while the cross-peaks were obtained from the ROESY experiments.

Conformational Searches Using NMR Data for Mortiamide D. The conformational search consisted in applying the LowModeMD sampling algorithm of MOE (https://www.chemcomp.com/Products.htm) to mortiamide D. As described by Labute,[8] this method is a stochastic conformation generation protocol based on the perturbation of a given 3D conformation along a molecular dynamics trajectory using initial atomic velocities with kinetic energy concentrated on the low-frequency vibrational modes, followed by energy minimization. It is appropriate for macrocycles, protein loops, and sterically or topologically hindered systems.

Before running the conformational search, the 2D structure of mortiamide D was constructed using Chemdraw (https://perkinelmerinformatics.com/products/research/chemdraw/), uploaded to the MOE (https://www.chemcomp.com/Products.htm) window, and converted to 3D using the standard configuration of the quickprep tool of MOE

https://doi.org/10.1021/acsomega.3c01206
ACS Omega 2023, 8, 25832−25838

(https://www.chemcomp.com/Products.htm). After, a script in the .svl format created *in-house* was run over the structure to ensure a unique numeration of the atoms in order to avoid repeated numbers. Then, one round of conformational search was performed restraining the distances corresponding to the assignments (3N, 5-2), (6-N, 1-N), and (3-2, 6-N) in Table 1. The restrains were introduced using the option: "Edit/Potential/Restrain" of the MOE main menu, and an energy cutoff of 10 kcal·mol^{-1} to enable broader sampling of conformations. The force field chosen for the conformational search was the AMBER10:EHT[10] with all interactions enabled, Born solvation model, and dielectric constant = 47.2, corresponding to DMSO, which was the solvent used to obtain the NMR data. The conformational search was performed using the LowModeMD sampling algorithm,[8] at the *csearch* function, with maximum interactions = 10 000, RMSD cutoff for similar structures = 0.25, MM interaction limit = 500, and RMS gradient of 0.005 kcal/mol·Å. The conformational search was set to end when no new conformation is found after 100 consecutive interactions.

The conformational search returned a databank.mdb file containing 80 conformers that were further submitted to analysis using the Compute/Molecule/Spectral_Analysis/Conformer_Distribution tool, available in the menu of the same databank.mdb file. A .txt file containing the distances corresponding to the 8 assignments in Table 1 was then uploaded into the Spectral Analysis window, and a search for conformers meeting those distances was performed by clicking on the calculate button. The best-adjusted conformer was selected for further MD simulations.

Searches for the Predominant Conformers of Mortiamides A−C. The mortiamide D predominant conformer obtained from LowModeMD conformational search was used to investigate the predominant conformers of mortiamides A−C. First, the side chains of this conformer were mutated accordingly, in order to generate the corresponding conformers of mortiamides A−C, using the protein build tool of MOE. Then, each conformer was submitted to MD simulation using the software NAMD[13] and the AMBER10:EHT[10] force field, following the protocol described in the next section.

MD Simulations. The MD simulations were prepared using the Compute/Simulations/Dynamics module of MOE (https://www.chemcomp.com/Products.htm). The software used to run the simulations was NAMD,[13] and the force field was AMBER10:EHT,[10] with a cutoff of 10 kcal·mol^{-1} for electrostatic interactions and a range between 8 and 10 kcal·mol^{-1} for VdW interactions. The conformers were centered in cubic boxes containing around 2000 water molecules (or 440 DMSO molecules for the MD simulation of mortiamide D in DMSO) and neutralized with NaCl ions. The margin distance to the box wall was set to 10 Å, the standard distance used by MOE for MD simulations of biological systems. The steps of simulations involved the first 10 ps of an energy minimization step followed by 100 ps of NPT and 200 ps of NVT. This simpler equilibration protocol, compared to what is expected for more flexible molecular systems, was possible since our systems are conformationally restricted and sampling problems as a consequence of bad equilibration are unlikely. After equilibration, production steps of 200 ns of free MD simulation were performed. The MD simulation results were analyzed using the md_analysis tool and the database viewer (DBV) menu of MOE (https://www.chemcomp.com/Products.htm). The graphs of the MD simulation results were generated using the software PRISM. Also, the reference geometries for the RMSD plots were the 3D inputs of the MD simulations.

■ ASSOCIATED CONTENT

Supporting Information

The Supporting Information is available free of charge at https://pubs.acs.org/doi/10.1021/acsomega.3c01206.

Chemical shifts obtained for the protons of the mortiamide D; ^{13}C NMR spectra of mortiamide D (Figure S1); COSY NMR spectra of mortiamide D (Figure S2); COSY NMR spectra of mortiamide D (Figure S3); HSQC−DEPT NMR spectra of mortiamide D (Figure S4); HMBC NMR spectra of mortiamide D (Figure S5); NOE NMR assignments of all of the mortiamide D H's atoms (Table S1); distances monitored in the theoretical studies of method 1 (Figure S6); comparison of distances (Table S2); RMSD variation of the mortiamide D's backbone during the MD simulation in water and DMSO (Figure S7); superposition of frames of the backbones of the predominant conformers of mortiamide D (Figure S8); plot of variation of the φ dihedral angles of mortiamide D's backbone during the MD simulation in water (Figure S9); RMSD variation of the mortiamides A−C during the MD simulation (Figure S10); superposition of frames of the backbones of the predominant conformers of mortiamides A−C, collected at each 1 ns of MD simulation (Figure S11); and plot of variation of the φ dihedral angles of mortiamides A−C backbones during the MD simulations (Figure S12) (PDF)

■ AUTHOR INFORMATION

Corresponding Author

Steven R. LaPlante − *INRS − Centre Armand-Frappier Santé Biotechnologie, Université de Québec, Laval, Quebec H7V 1B7, Canada*; Email: Steven.LaPlante@inrs.ca

Authors

Tanos C. C. Franca − *INRS − Centre Armand-Frappier Santé Biotechnologie, Université de Québec, Laval, Quebec H7V 1B7, Canada; Laboratory of Molecular Modeling Applied to Chemical and Biological Defense, Military Institute of Engineering, 22290-270 Rio de Janeiro, Brazil; Department of Chemistry, Faculty of Science, University of Hradec Králové, 50003 Hradec Králové, Czech Republic;* orcid.org/0000-0002-6048-8103

Arlan da Silva Goncalves − *Department of Chemistry, Federal Institute of Espírito Santo − Unit Vila Velha, 29106-010 Vila Velha, ES, Brazil; PPGQUI (Graduate Program in Chemistry), Federal University of Espírito Santo, 29075-910 Vitória, ES, Brazil*

Christopher Bérubé − *Departement de Chimie and PROTEO, Faculté des Sciences et de Génie, Université Laval, Québec, Quebec G1V OA6, Canada*

Normand Voyer − *Departement de Chimie and PROTEO, Faculté des Sciences et de Génie, Université Laval, Québec, Quebec G1V OA6, Canada;* orcid.org/0000-0002-0429-9172

https://doi.org/10.1021/acsomega.3c01206
ACS Omega 2023, 8, 25832−25838

Norman Aubry − *NMR consultant of Steven R. LaPlante's Lab, INRS − Centre Armand-Frappier Santé Biotechnologie, Université de Québec, Laval, Quebec H7V 1B7, Canada*

Complete contact information is available at: https://pubs.acs.org/10.1021/acsomega.3c01206

Author Contributions

C.B. and N.V. prepared the sample of mortiamide D; S.R.L. and N.A. acquired and analyzed the NMR data; A.d.S.G., T.C.C.F., and N.A. performed the conformational search studies; T.C.C.F. ran and analyzed the MD simulations; T.C.C.F. drafted the manuscript; and S.R.L. provided revisions.

Notes

The authors declare no competing financial interest.

■ ACKNOWLEDGMENTS

The authors thank the following for their support: CQDM SynergiQc project, Mitacs, NSERC, CFI, PROTEO, and NMX Research and Solutions, Inc., FAPES-BPC-Pq (grand number 06/2021), IFES-PRPPG (grant number 12/2020 - Researcher Productivity Program, PPP) and FAPES (grant number 03/2020-2020-WMT5F). This work was also supported by the Excellence project PřF UHK 2216/2023−2024.

■ REFERENCES

(1) Grunwald, A. L.; Berrue, F.; Robertson, A. W.; Overy, D. P.; Kerr, R. G. Mortiamides A−D, cyclic heptapeptides from a novel Mortierella sp. obtained from Frobisher Bay. *J. Nat. Prod.* **2017**, *80*, 2677−2683.

(2) (a) Baraguey, C.; Blond, A.; Cavelier, F.; Pousset, J.-L.; Bodo, B.; Auvin-Guette, C. Isolation, structure and synthesis of mahafacyclin B, a cyclic heptapeptide from the latex of Jatropha mahafalensis. *J. Chem. Soc., Perkin Trans. 1* **2001**, 2098−2103. (b) Van den Berg, A.; Horsten, S.; Kettenes-Van Den Bosch, J.; Kroes, B.; Beukelman, C.; Leeflang, B.; Labadie, R. Curcacycline A—a novel cyclic octapeptide isolated from the latex of Jatropha curcas L. *FEBS Lett.* **1995**, *358*, 215−218.

(3) Bérubé, C.; Gagnon, D.; Borgia, A.; Richard, D.; Voyer, N. Total synthesis and antimalarial activity of mortiamides A−D. *Chem. Commun.* **2019**, *55*, 7434−7437.

(4) Appavoo, S. D.; Huh, S.; Diaz, D. B.; Yudin, A. K. Conformational Control of Macrocycles by Remote Structural Modification: Focus Review. *Chem. Rev.* **2019**, *119*, 9724−9752.

(5) (a) Wüthrich, K.; Tun-Kyi, A.; Schwyzer, R. Manifestation in the 13C-NMR spectra of two different molecular conformations of a cyclic pentapeptide. *FEBS Lett.* **1972**, *25*, 104−108. (b) Rowan, R., III; Warshel, A.; Skyes, B.; Karplus, M. Conformation of retinal isomers. *Biochemistry* **1974**, *13*, 970−981. (c) De Leeuw, F. A. A. M.; Altona, C.; Kessler, H.; Bermel, W.; Friedrich, A.; Krack, G.; Hull, W. E. Peptide conformations. 20. Conformational analysis of proline rings from proton spin-spin coupling constants and force-field calculations: application to three cyclic tripeptides. *J. Am. Chem. Soc.* **1983**, *105*, 2237−2246. (d) Scarsdale, J. N.; Yu, R.; Prestegard, J. Structural analysis of a glycolipid head group with one-and two-state NMR pseudoenergy approaches. *J. Am. Chem. Soc.* **1986**, *108*, 6778−6784. (e) Kessler, H.; Griesinger, C.; Lautz, J.; Mueller, A.; Van Gunsteren, W. F.; Berendsen, H. J. Conformational dynamics detected by nuclear magnetic resonance NOE values and J coupling constants. *J. Am. Chem. Soc.* **1988**, *110*, 3393−3396. (f) Yangmee, K.; Ohlrogge, J. B.; Prestegard, J. H. Motional effects on NMR structural data: comparison of spinach and Escherichia coli acyl carrier proteins. *Biochem. Pharmacol.* **1990**, *40*, 7−13. (g) Kopple, K. D.; Baures, P. W.; Bean, J. W.; D'Ambrosio, C. A.; Hughes, J. L.; Peishoff, C. E.; Eggleston, D. S. Conformations of Arg-Gly-Asp containing heterodetic cyclic peptides: solution and crystal studies. *J. Am. Chem. Soc.* **1992**, *114*, 9615−9623. (h) Hickey, J. L.; Zaretsky, S.; St Denis, M. A.; Kumar Chakka, S.; Morshed, M. M.; Scully, C. C.; Roughton, A. L.; Yudin, A. K. Passive membrane permeability of macrocycles can be controlled by exocyclic amide bonds. *J. Med. Chem.* **2016**, *59*, 5368−5376.

(6) (a) Müller, G.; Gurrath, M.; Kessler, H.; Timpl, R. Dynamic Forcing, a Method for Evaluating Activity and Selectivity Profiles of RGD (Arg-Gly-Asp) Peptides. *Angew. Chem., Int. Ed.* **1992**, *31*, 326−328. (b) Cuniasse, P.; Raynal, I.; Yiotakis, A.; Dive, V. Accounting for conformational variability in NMR structure of cyclopeptides: ensemble averaging of interproton distance and coupling constant restraints. *J. Am. Chem. Soc.* **1997**, *119*, 5239−5248. (c) Nikiforovich, G.; Vesterman, B.; Betins, J. Combined use of spectroscopic and energy calculation methods for the determination of peptide conformation in solution. *Biophys. Chem.* **1988**, *31*, 101−106. (d) Nikiforovich, G. V.; Kövér, K. E.; Zhang, W.-J.; Marshall, G. R. Cyclopentapeptides as flexible conformational templates. *J. Am. Chem. Soc.* **2000**, *122*, 3262−3273.

(7) (a) Hawkins, P. C. D. Conformation generation: the state of the art. *J. Chem. Inf. Model.* **2017**, *57*, 1747−1756. (b) Foloppe, N.; Chen, I.-J. Conformational sampling and energetics of drug-like molecules. *Curr. Med. Chem.* **2009**, *16*, 3381−3413. (c) Shim, J.; MacKerell Jr, A. D. Computational ligand-based rational design: role of conformational sampling and force fields in model development. *MedChemComm* **2011**, *2*, 356−370. (d) Coutsias, E. A.; Lexa, K. W.; Wester, M. J.; Pollock, S. N.; Jacobson, M. P. Exhaustive Conformational Sampling of Complex Fused Ring Macrocycles Using Inverse Kinematics. *J. Chem. Theory Comput.* **2016**, *12*, 4674−4687. (e) Bonnet, P.; Agrafiotis, D. K.; Zhu, F.; Martin, E. Conformational analysis of macrocycles: finding what common search methods miss. *J. Chem. Inf. Model.* **2009**, *49*, 2242−2259.

(8) Labute, P. LowModeMD - implicit low-mode velocity filtering applied to conformational search of macrocycles and protein loops. *J. Chem. Inf. Model.* **2010**, *50*, 792−800.

(9) Sindhikara, D.; Spronk, S. A.; Day, T.; Borrelli, K.; Cheney, D. L.; Posy, S. L. Improving Accuracy, Diversity, and Speed with Prime Macrocycle Conformational Sampling. *J. Chem. Inf. Model.* **2017**, *57*, 1881−1894.

(10) Case, D. A.; Darden, T.; Cheatham, T.; Simmerling, C. L.; Wang, J.; Duke, R. E.; Luo, R.; Crowley, M.; Walker, R. C.; Zhang, W. *Amber 10*; University of California, 2008.

(11) (a) LaPlante, S. R.; Bös, M.; Brochu, C.; Chabot, C.; Coulombe, R.; Gillard, J. R.; Jakalian, A.; Poirier, M.; Rancourt, J.; Stammers, T.; et al. Conformation-based restrictions and scaffold replacements in the design of hepatitis C virus polymerase inhibitors: discovery of deleobuvir (BI 207127). *J. Med. Chem.* **2014**, *57*, 1845−1854. (b) LaPlante, S. R.; Nar, H.; Lemke, C. T.; Jakalian, A.; Aubry, N.; Kawai, S. H. Ligand bioactive conformation plays a critical role in the design of drugs that target the hepatitis C virus NS3 protease. *J. Med. Chem.* **2014**, *57*, 1777−1789.

(12) Oguadinma, P.; Bilodeau, F.; LaPlante, S. R. NMR strategies to support medicinal chemistry workflows for primary structure determination. *Bioorg. Med. Chem. Lett.* **2017**, *27*, 242−247.

(13) Nelson, M. T.; Humphrey, W.; Gursoy, A.; Dalke, A.; Kalé, L. V.; Skeel, R. D.; Schulten, K. NAMD: a parallel, object-oriented molecular dynamics program. *Int. J. Supercomput. Appl. High Performance Comput.* **1996**, *10*, 251−268.